RESEARCH ARTICLE

Dynamic contrast-enhanced MR in the diagnosis of lympho-associated benign and malignant lesions in the parotid gland

[1]Ling Zhu, [2]Chunye Zhang, [3]Yi Hua, [4]Jie Yang, [1]Qiang Yu, [1]Xiaofeng Tao and [5]Jiawei Zheng

[1]Department of Radiology, Ninth People's Hospital, School of Medicine, Shanghai Jiao Tong University, Shanghai, China;
[2]Department of Oral pathology, Ninth People's Hospital, School of Medicine, Shanghai Jiao Tong University, Shanghai, China;
[3]Department of prevention and health care, Preventive and health care center of Wuzhong economic developing-area, Suzhou, China; [4]Division of Oral & Maxillofacial Radiology, Temple University School of Dentistry, and Department of Diagnostic Imaging, Temple University School of Medicine, PA, USA; [5]Department of Oral and Maxillofacial Surgery, Ninth People's Hospital, School of Medicine, Shanghai Jiao Tong University, Shanghai, China

Objective: The aim of this study was to determine if dynamic contrast-enhanced (DCE)-MRI can differentiate mucosa-associated lymphoid tissue (MALT) lymphoma from benign lymphoepithelial lesion (BLEL) in the parotid gland.
Methods: 25 patients with tumour-like BLEL and 20 patients with MALT lymphoma in the parotid gland confirmed by pathology were examined pre-operatively using routine MR series and DCE-MRI with a 1.5-T MR unit. The time to peak (TTP), time to start (TTS), SI_{start}, SI_{max} and SI_{ending} were measured and the initial slope of increase (ISI) and relative washout ratio (RWO) were calculated separately from the time–intensity curve (TIC), and the types of TIC were analysed.
Results: There were significant differences in the TTP and ISI between the two lesions ($p < 0.001$). The sensitivity, specificity and accuracy of TTP were all more than 90%. TICs were divided into three types according to the threshold of TTP and ISI: tumour-like BLEL: gradual type (Type II) and late increase type (Type III); MALT lymphoma: rapid increase and gradual type (Type I).
Conclusions: DCE-MRI contributed greatly to the differential diagnosis between tumour-like BLEL and MALT lymphoma in the parotid gland.
Dentomaxillofacial Radiology (2016) **45**, 20150343. doi: 10.1259/dmfr.20150343

Cite this article as: Zhu L, Zhang C, Hua Y, Yang J, Yu Q, Tao X, et al. Dynamic contrast-enhanced MR in the diagnosis of lympho-associated benign and malignant lesions in the parotid gland. *Dentomaxillofac Radiol* 2016; **45**: 20150343.

Keywords: DCE-MRI; parotid gland; BLEL; MALT lymphoma

Introduction

A normal parotid tissue contains almost no mucosa-associated lymphoid tissue (MALT). However, in chronic inflammatory or autoimmune disease of the parotid gland, such as benign lymphoepithelial lesion (BLEL), there could be aggregation and proliferation of the lymphoid tissue, thereby leading to acquired MALT. Research has found that amongst patients with BLEL, approximately 4–7% developed lymphomas.[1] The risk for the occurrence of lymphoma in this patient group is 44 times higher than that in the general population, of which 85% are MALT lymphomas.[2–4] Therefore, timely and accurate differentiation between parotid BLEL and MALT lymphoma is the key to the treatment selection and prognostic evaluation of patients. Parotid BLELs are usually categorized as diffused, atrophic, tumour-like and infectious types.[5] The diffused, atrophied and infectious types lack solid lumps or nodules; thus, they are easily distinguished from parotid BLEL based on conventional imaging. However, tumour-like BLEL cannot be distinguished from MALT lymphoma using conventional CT or MRI morphologically.[6,7]

Recently, interest has been growing in tumour functional MRI, such as MR spectroscopy (MRS),[8,9] diffusion-weighted (DW)-MRI[10,11] and dynamic contrast-enhanced (DCE)-MRI,[12–14] because of improvements in the accuracy of detection and characterization. DCE-MRI reflects the density, intensity and leakiness of the tumour vasculature. The parameters calculated from DCE-MRI are used to assess the histological properties of the tumour, since vessels produced by angiogenesis are leaky and incompletely formed. But, so far, DCE-MRI has not been used to differentiate between benign parotid tumour-like BLEL and MALT lymphoma.

This study was to investigate whether DCE-MRI can add important information to distinguish MALT lymphoma from BLEL in the parotid gland. The time–intensity curve (TIC) and parameters obtained from the TIC were analysed.

Methods and materials

Ethics statement
This retrospective study was approved by the Ethics Committee of the Shanghai Ninth Hospital affiliated to the Shanghai Jiaotong University School of Medicine (No. 2015-121), and written informed consent were obtained from all the subjects.

Patients
25 patients with parotid tumour-like BLEL and 20 patients with parotid MALT lymphoma were admitted and treated in our hospital between January 2003 and November 2013 and were included in the study.

The chief complaints of the 16 patients with parotid tumour-like BLEL (64%) and 12 patients with parotid MALT (60%) were keratoconjunctivitis sicca, xerostomia and other symptoms of Sjögren's syndrome. 20 patients experienced swelling around the parotid gland, but all were without pain or facial paralysis. Immobile, moderately firmed, painless and palpable masses were found during clinical examinations in 10 patients with parotid tumour-like BLEL and 11 patients with MALT lymphoma.

MRI examination
A 1.5-T MR scanner (Sigma MRI, GE Medical System, Milwaukee, WI) was used in this study, with head and neck array coils. T_1 and T_2 series consisted of 5-mm section thickness and 1-mm intersection gap, 228×192 acquisition matrix and 24×18-cm field of view (FOV). Transverse T_1 weighted spin time (SE) sequences were performed with a repetition time (TR) of 400 ms and echo time (TE) of 8 ms. Transverse T_2 weighted fast spin-echo (FSE) sequences were performed with a TR of 4.020 ms and TE of 84.8 ms.

Parotid tumours were identified on transverse T_1 weighted MR images, and three sections (one section accounted for the maximum diameter or highest number of nodules of the tumour) were selected for DCE imaging. FSE T_1 weighted images were obtained with a TR of 400–600 ms and TE of 8–9.9 ms. Gadolinium diethylenetriamine pentaacetic acid (Gd-DTPA) (Magnevist®, Schering, Berlin, Germany) was administered intravenously at a rate of $2 \, \text{ml s}^{-1}$ (total dose, 0.1 mmole per kg of body weight) using a power injector, followed by a 20-ml saline flush. DCE images were sequentially obtained prior to and at 0, 30, 60, 90, 120, 150, 180, 210, 240, 270 and 300 s, following administration of contrast material. The total acquisition time was approximately 8 min.

MRI evaluation
Based on the morphology of the tumour in routine MRI, parotid tumour-like BLEL and MALT lymphoma were classified into solitary-nodule type and multiple-nodule type. The section with the maximum diameter or the highest number of nodules was selected as the central section, and additional sections 1.25 cm above and below were also selected. The region of interest was manually depicted by a radiologist (12 years' experience in head and neck MRI), who was blinded to clinical information and histopathological results, and determined all relevant points, and covered the major lesion region as much as possible.

After the TIC was constructed, raw parameters such as SI_{start}, time to start (TTS), SI_{max}, time to peak (TTP) and SI_{ending} were measured. SI_{start} represented the pre-contrast signal intensity. SI_{max} was obtained as the signal intensity at maximal contrast enhancement, and SI_{ending} as the SI of the ending point. SI_{peak} was defined as the first SI measurement that satisfied the inequality $SI > [0.9 \, (SI_{max} - SI_{start})] + SI_{start}$. TTS and TTP represented the time that corresponded with the SI_{start} and SI_{peak}, respectively. The initial slope of increase (ISI) and relative washout (RWO) values were calculated using the following formulas: $ISI = (SI_{peak} - SI_{start})/(TTP - TTS)$ and $RWO = (SI_{max} - SI_{ending})/SI_{max} \times 100\%$.

Statistical analysis
The SPSS® 10.0 statistical software package (IBM Corp., New York, NY; formerly SPSS Inc., Chicago, IL: 1999) was used, and the unpaired t-test was used to compare the TIC parameters of BLEL with those of MALT lymphoma. A probability of p-value <0.05 showed a statistically significant difference. The Youden Index was used to determine the optimized threshold value, which was further used to calculate the sensitivity, specificity and accuracy. A global measure of biomarker effectiveness is the Youden Index, the maximum difference between sensitivity, the probability of correctly classifying diseased individuals and 1-specificity, the probability of incorrectly classifying healthy individuals.

Results

Patients

38 patients underwent DCE-MRI successfully, and 7 patients were excluded owing to the tumour being <10 mm in diameter or random movement. 21 patients (2 males and 19 females aged 19–74 years, mean age of 52.1 years) had parotid tumour-like BLEL and 17 patients (5 males and 12 females, aged 32–76 years, mean age of 54.7 years) had parotid MALT lymphoma.

Analysis of measured parameters from TIC (SI_{start}, TTS, SI_{max}, TTP and SI_{ending})

The averaged parameters of SI_{start}, TTS, SI_{max}, TTP and SI_{ending} measured from the TIC of the parotid tumour-like BLEL and MALT lymphoma are presented in Table 1. (1) The SI_{start} of the two groups showed that parotid tumour-like BLEL parameters were slightly higher than those of MALT lymphoma, but the difference was not statistically significant. (2) In these two groups, TTS indicated that parotid MALT lymphoma appeared slightly earlier than tumour-like BLEL; however, both below 60s. The difference was not statistically significant. (3) SI_{max} revealed that the signal of the parotid MALT lymphoma was slightly higher than that of the tumour-like BLEL. The difference was not statistically significant. (4) The TTP of the parotid tumour-like BLEL was more than twice as that of the MALT lymphoma, with statistically significant difference. (5) SI_{ending} showed that there was no significant difference in these two lesions, and SI_{ending} of MALT lymphoma was slightly higher than that of the tumour-like BLEL.

Only TTP had a significant difference among the five groups, and the area measured under the receiver-operating characteristic (ROC) curve was 0.987. According to the Youden Index, the optimal threshold was 79.65s (Figure 1a). According to this threshold, tumour TTP value greater than 79.65s indicated parotid BLEL (negative), and tumour TTP value below 79.65s indicated MALT lymphoma (positive). The negative rate calculated for parotid tumour-like BLEL was 95.2% (20/21 patients), and only 1 patient presented a TTP value greater than 79.65s (false positive). The positive rate of parotid MALT lymphoma was 94.1%, and only one patient presented a TTP value greater than the threshold value (false negative). Based on this TTP threshold value, the sensitivity rate, specificity rate and accuracy rate of differential diagnosis was 94.1%, 95.2% and 94.7%, respectively, between parotid tumour-like BLEL and MALT lymphoma.

Analysis of the initial slope of increase and relative washout ratio

Parameter analysis indicated that the average ISI value of parotid MALT lymphoma was 1.67, which was much larger than that of BLEL (ISI = 0.465). There was significant difference between the two groups. ($p < 0.001$) (Figure 2a). The average RWO value of the parotid MALT lymphoma (9.4%) was greater than that of the tumour-like BLEL (6.1%). The difference between the two groups was not statistically significant ($p = 0.254$, $p > 0.05$) (Figure 2b).

The ROC curve of ISI exhibited that the area under the curve was 0.950. The optimal threshold value prompted according to the Youden Index was 0.807 (Figure 1b). Based on this threshold, it was assumed that ISI> 0.807 indicates parotid MALT lymphoma (positive) and ISI<0.807 indicates tumour-like BLEL (negative). Among the 21 cases of patients with parotid tumour-like BLEL, the ISI values of 5 patients were greater than the threshold value, which indicated false positive. Among the 17 cases of patients with parotid MALT lymphoma, the ISI values of 3 cases were lower than the threshold value, which indicated false negative. When the ISI threshold value was 0.807, the sensitivity rate was 82.3%, specificity rate was 76.2% and accuracy rate was 78.9%.

Analysis of time–intensity curve types

Only two parameters (measured TTP and calculated ISI) achieved statistical significance. The threshold value of TTP was 79.65s and that of ISI was 0.807. According to these two optimal threshold values, we proposed that the TIC should be divided into three types: Type I (rapid increase and gradual type), TTP <79.65s, ISI> 0.807 (Figure 3, a–b); Type II (gradual type), TTP> 79.65s, ISI <0.807 (Figure 4a–b); and Type III (late increase type), TTP> 79.65s, ISI> 0.807 (Figure 5a–b). Parotid tumour-like BLEL mainly presented as Type II and Type III, mainly as Type II (16/21 patients, 76.2%); parotid MALT lymphoma mainly

Table 1 The parameters of SI_{start}, TTS, SI_{max}, TTP, SI_{ending}, ISI and RWO from TIC

BLEL/MALT lymphoma	SI_{start}	TTS(s)	SI_{max}	TTP(s)	SI_{ending}	ISI	RWO
Average value							
BLEL	49.0	23.9	100.4	157.3	93.6	0.5	6.1
Mean ± SD							
MALT lymphoma	46.1	24.4	109.3	65.4	98.6	1.7	9.4
BLEL	49.0 ± 6.1	23.9 ± 7.5	100.4 ± 14.0	157.3 ± 44.3	93.6 ± 14.1	0.5 ± 0.3	6.1 ± 11.8
MALT lymphoma	46.1 ± 10.5	24.4 ± 3.1	109.3 ± 21.5	65.4 ± 10.1	98.6 ± 18.2	1.7 ± 0.7	9.4 ± 4.8
p-value	0.293	0.807	0.154	<0.001	0.356	<0.001	0.254

BLEL, benign lymphoepithelial lesion; ISI, initial slope of increase; MALT, mucosa-associated lymphoid tissue; RWO, relative washout ratio; SD, standard deviation; SI_{ending}, SI of ending point; TTP, time to peak; TTS, time to start.
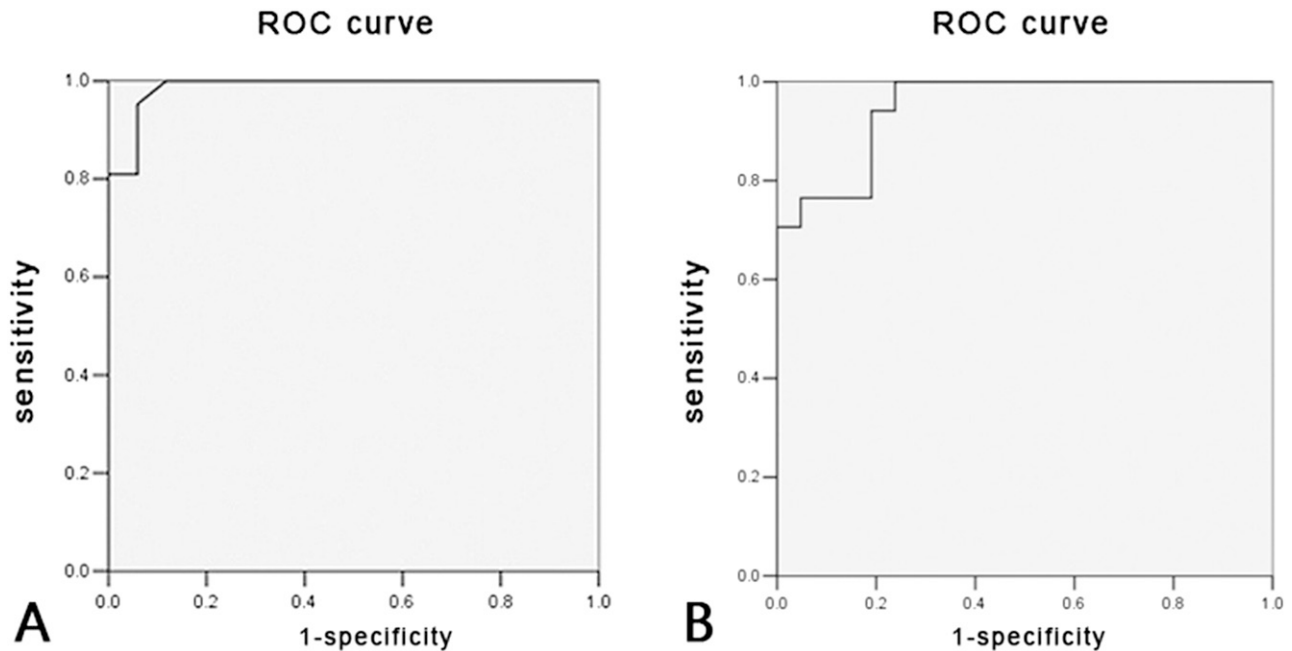
Figure 1 (a) The receiver-operating characteristic (ROC) of time to peak; the area under the ROC curve was 0.987. (b) The ROC of the initial slope of increase; the area under the ROC curve was 0.950.

presented as Type I (16/17 patients, 94.1%). In 1 case of parotid tumour-like BLEL, TIC presented as Type I (1/21 patients, 5%). One case of parotid MALT lymphoma presented as Type II (1/17 patients, 6%). It was assumed that Type I of TIC was parotid MALT lymphoma (positive) and Type II or Type III was parotid tumour-like BLEL (negative). The sensitivity rate was 94.1%, specificity rate was 95.2% and accuracy rate was 94.7%. The assumed hypothesis that TTP lower than threshold indicated parotid MALT lymphoma was confirmed.

Discussion

Analysis of the application of dynamic contrast-enhanced MR in the tumour of the salivary gland

At present, the clinical application of MRI has outgrown the simple use of basic information such as location, shape and signal intensity to evaluate the nature of the lesion. The employment of functional MRI technology for the evaluation of disease is maturing, and the clinical application is becoming more and more common.[15–19] DCE-MRI is one of the most
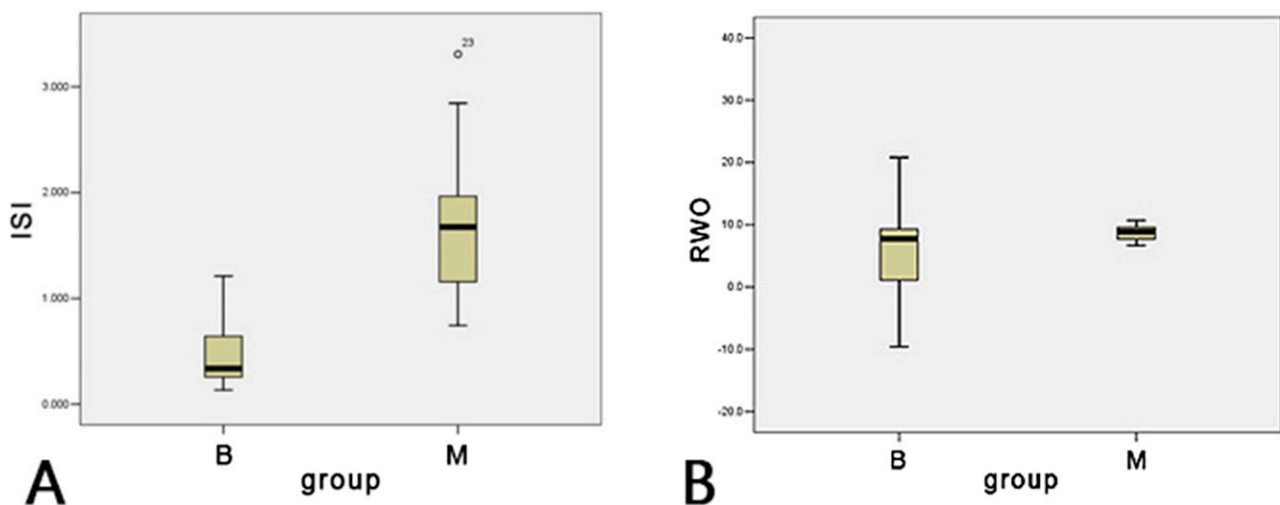

Figure 2 There was a significant difference in the initial slope of increase (ISI) (a) ($p < 0.001$) and no significant difference in the relative washout ratio (RWO) (b) ($p > 0.05$) of two lesions. B, benign lymphoepithelial lesion, M, mucosa-associated lymphoid tissue lymphoma.
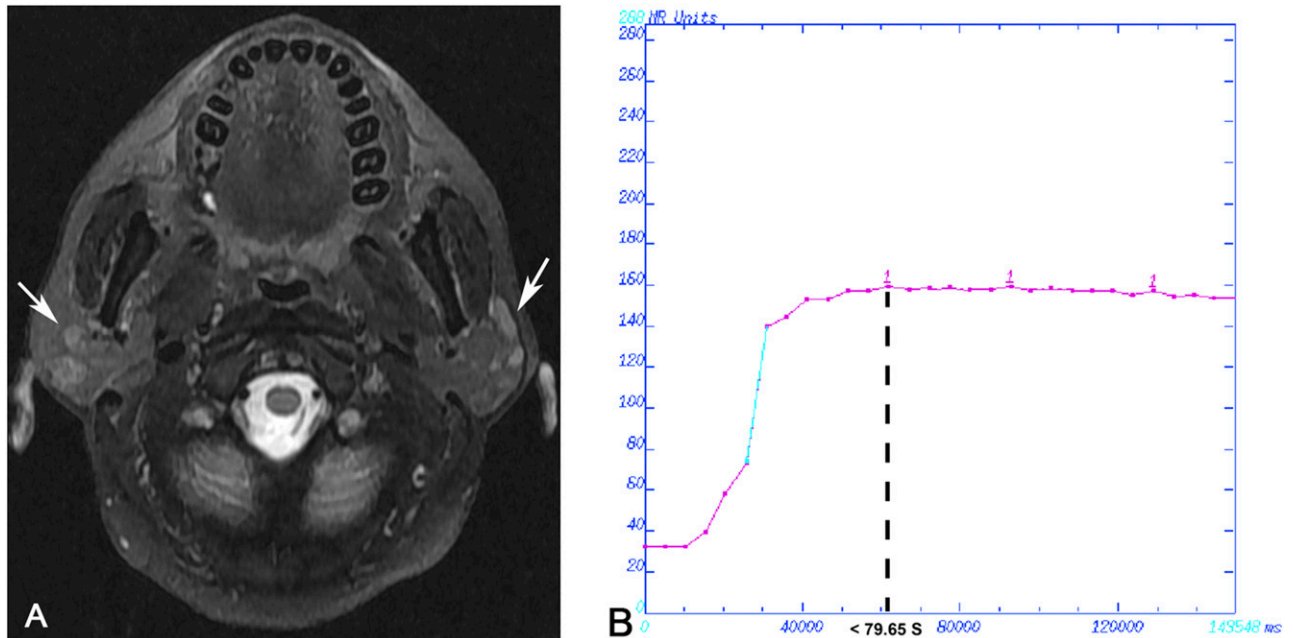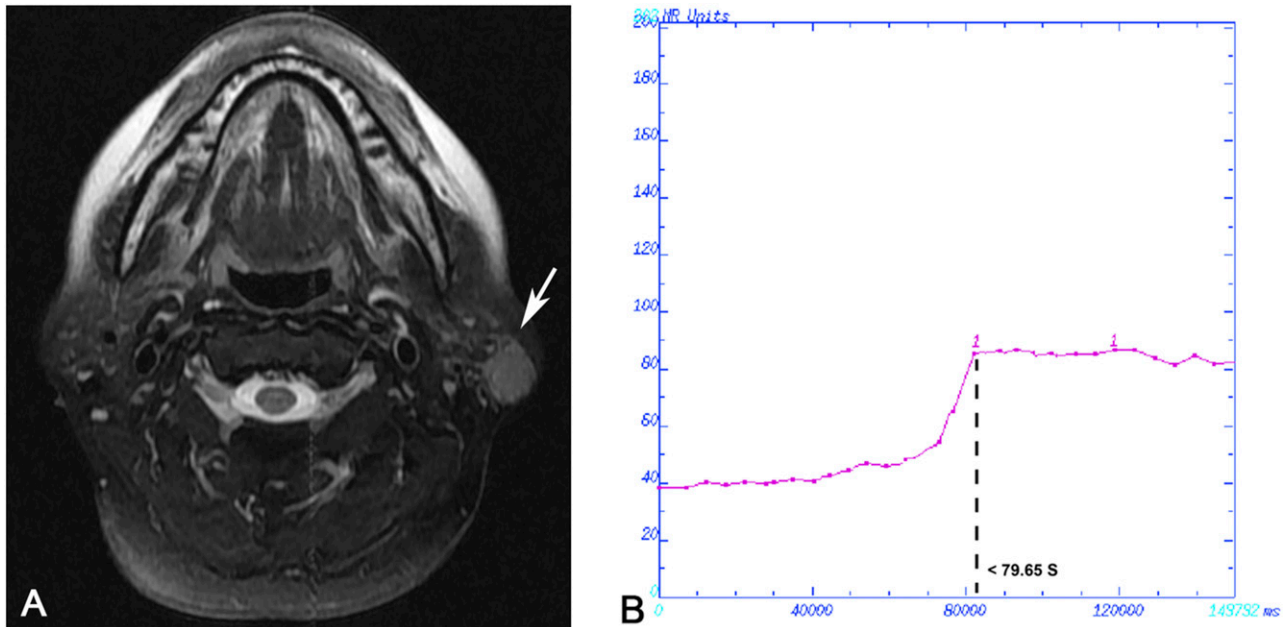
Figure 3 Case 1: Mucosa-associated lymphoid tissue lymphoma in a 51-year-old female analysed by dynamic contrast-enhanced MRI. (a) Transverse T_2 weighted spin time MRI showing heterogeneously hyperintense multiple nodules in the parotid gland bilaterally (arrows). The region of interest was chosen in the section with the highest number of nodules in the right side, and the whole gland was included. (b) Time–intensity curve shown as Type I, rapid increase and gradual type.

widely used and most developed functional MRI techniques and is also among the most mature ones in the field of exogenous tracer perfusion imaging technologies.[20]

The literature review[21–23] showed that: malignant tumour and normal tissue of the head and neck could be distinguished; malignant lymphoma and other lymph nodes could be differentiated.
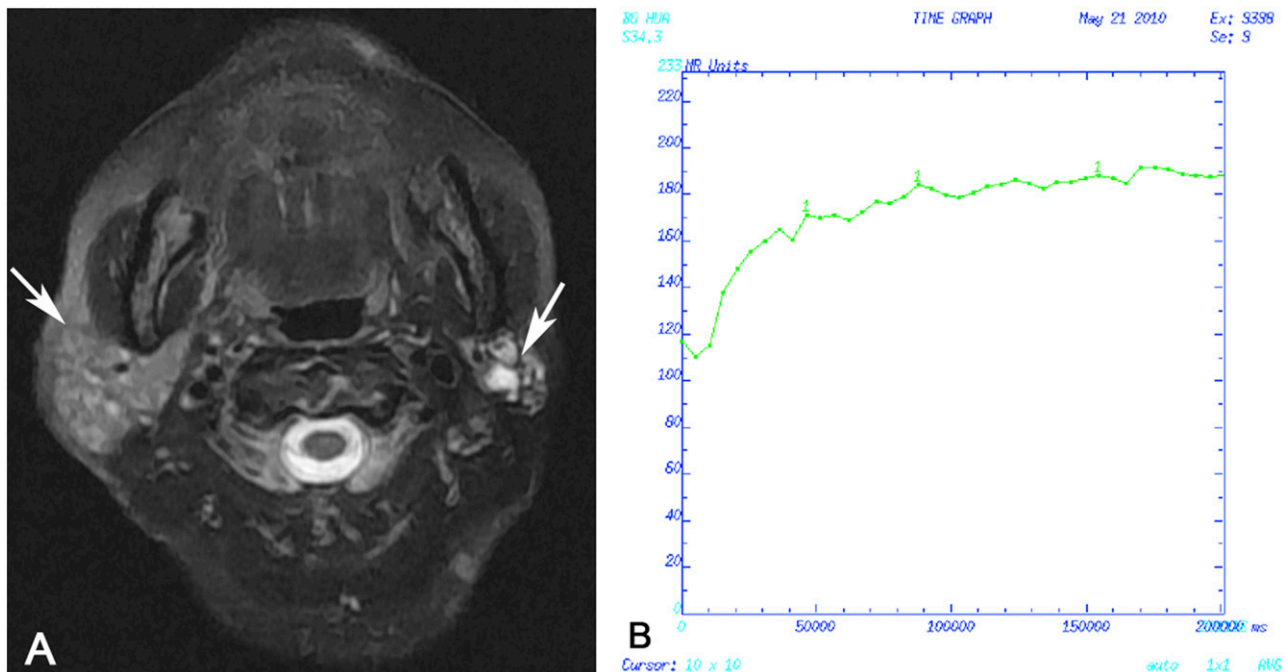
Figure 4 Case 2: Tumour-like benign lymphoepithelial lesion in a 27-year-old female analysed by dynamic contrast-enhanced MRI. (a) Transverse T_2 weighted spin time MRI showing heterogeneously hyperintense multiple nodules in the parotid gland bilaterally (arrows). The features of routine MRIs are similar between Case 1 and Case 2. The region of interest was chosen in the section with the highest number of nodules in the right side, and the whole gland was included. (b) Time–intensity curve shown as Type II, gradual type.

6 of 9
Application of DCE-MRI in parotid BLEL and MALT lymphoma
Zhu *et al*

Figure 5 Case 3: Tumour-like benign lymphoepithelial lesion in a 49-year-old female analysed by dynamic contrast-enhanced MRI. (a) Transverse T_2 weighted spin time MRI showing a heterogeneously hyperintense solitary nodule in the left parotid gland (arrow). (b) Time–intensity curve shown as Type III, late increase type.

During the DCE-MR inspection of the primary head and neck tumour, it was found that the TIC of malignant lymphoma was wash-in and washout type, and it was proposed that this feature of the curve was in favour of being distinguishing from the other primary head and neck tumours. Asaumi et al[24] found that the squamous-cell carcinoma (SCC) had a shorter peak time and higher SI_{max} than the malignant lymphoma in the head and neck, with statistically significant differences. The incidence of malignant lymphoma is increasing among malignant tumours in the head and neck, and it is important to make a different diagnosis in order to make a proper treatment plan. Yabuuchi et al[25] discovered that malignant tumour and parotid Warthin's tumour had the same TIC type (wash-in and washout type), and peak times were not statistically different. Although it is difficult to distinguish between malignant tumour and Warthin's tumour on the basis of TICs alone, these features can help in distinguishing them from other tumours.

The application of DCE-MR in cases of parotid primary tumours has previously been reported. Takashima et al[26] divided TICs into five types according to the T_{peak} after injection of the contrast agent. Tsushima et al indicated that the SI of seven cases of pleomorphic adenoma (PLA) and two cases of adenoid cystic carcinoma (ACC) presented gradually enhanced after 260s, the SI of Warthin's tumour decreased significantly after fast enhancement in 20s, the SI of malignant tumour clearly enhanced after 20s, then gradually decreased or continued enhancing. Therefore, DCE-MRI may be useful to distinguish between PLA and Warthin's tumour; however, it cannot be useful to differentiate PLA from ACC or Warthin's tumour from malignant tumour. In addition, using T_{peak} and combined with other multiTIC parameters, Yabuuchi et al[27] diagnosed and analysed primary benign and malignant parotid tumour. They found that the parotid PLA and malignant tumour could be differentiated when T_{peak} was 120s (assumed as PLA, $T_{peak} > 120s$). However, parotid Warthin's tumour could not be distinguished from malignant tumour only by T_{peak}. The washout ratio (WR) of Warthin's tumour was significantly higher than that of malignant tumours, and the difference between them was statistically significant. Therefore, through the combination of T_{peak} and WR, differential diagnosis of parotid PLA, Warthin's tumour and malignant tumour could be made. Longer T_{peak} indicated PLA, shorter T_{peak} with higher WR indicated Warthin's tumour and shorter T_{peak} with lower WR indicated malignant tumour. However, the differences of enhancement ratio (ER) in tumours were not statistically significant and were useless for differential diagnosis. After analysis and research of TIC types and parameters of parotid tumour, Hisatomi et al[12] concluded that DCE-MR parameters could provide important information for the differential diagnosis of parotid primary benign and malignant tumours, and the combination of T_{max} and WR had the largest significance in differential diagnosis between the tumours. Matsuzaki et al[28] reported that DCE-MRI parameters had less significance in the differential diagnosis of small salivary gland tumours than in that of large salivary gland tumours. In the differential diagnosis of various types of small salivary gland

tumours, T_{max} had larger significance in the differential diagnosis of benign and malignant tumours. Based on the literature review above as well as the results of the present study, we selected TTP and ISI to conduct differential diagnosis between parotid tumour-like BLEL and MALT lymphoma and analysed the significance of these two parameters in the differential diagnosis.

Parameter analysis of SI_{start}, TTS, SI_{max}, TTP and SI_{ending}

Maybe it is hard to make the consistent and repeatable definition, the application of SI_{start} for differential diagnosis of tumours has not been reported yet. Generally, SI_{start} is set to the lowest point of the enhancing peak. This study found that the difference in SI_{start} and TTS was not statistically significant between parotid tumour-like BLEL and MALT lymphoma and could not contribute any useful information. The mean TTS values of parotid tumour-like BLEL and MALT lymphoma were both less than 30s; but, for four tumour-like BLEL and only one MALT lymphoma's, TTS were longer than 30s. The difference of SI_{max} and SI_{ending} was not statistically significant in parotid tumour-like BLEL and MALT lymphoma, which indicated that SI_{max} and SI_{ending} could not provide insight for the differential diagnosis of the two lesions.

The mean TTP value of parotid MALT lymphoma was only 65.4s, while that for tumour-like BLEL, it was 157.3s, more than twice as large as the former. Yabuuchi et al[27] discovered that mean the TTP value of PLA was greater than 210s; TTP values were often less than 60s for Warthin's tumour and malignant lymphoma. Early enhancing performance of the tumours is related to their degrees of vascularization. The malignant tumours, with higher degree of vascularization, usually present as early strengthening. The TTP value of parotid MALT lymphoma was 56.4s, in accordance with its low-grade malignant feature pathologically. The TTP value of parotid tumour-like BLEL was 157.3s (>120s), generally considered as late strengthening, and could be differentiated from malignant tumours and the PLA (210s). Thus, TTP can provide important information for the differential diagnosis of parotid tumour-like BLEL and MALT lymphoma, which can reflect the pathological features of the benign and malignant lesions, respectively.

Analysis of calculated parameters (initial slope of increase and relative washout ratio)

The difference in ISI of parotid tumour-like BLEL and MALT lymphoma was statistically significant. It was smaller in BLEL (ISI = 0.464) while larger in MALT lymphoma (ISI = 1.671), which indicated that the strengthening speed of MALT lymphoma was much greater than that of tumour-like BLEL. ISI also reflects the enhancing degree of lesions in the early stage, as well as perfusion information. The lesion with high degree of vascularization and rich perfusion performs a steep slope and early peak in TIC; otherwise, it shows little

slope and late peak. The steep slope and early peak of parotid MALT lymphoma reflected its features as high degree of vascularization and rich perfusion of vascular, which could differentiate it from tumour-like BLEL and had great diagnostic significance.

Yabuuchi et al[25] found that RWO could provide important information for differential diagnosis in parotid tumours (PLA, Warthin's tumour and malignant tumour). WR_{300} of PLA was <10%, Warthin's tumour was >40%, while malignant tumours ranged from 10% to 30%. Late stage of enhancement was usually correlated with vascular permeability and the osmotic pressure difference between tumour and stroma. Stronger vascular permeability and larger osmotic pressure led to greater RWO value of malignant tumours. The study found that RWO values of the parotid tumour-like BLEL and MALT lymphoma were both small (<10%). This phenomenon might be related to the low-grade malignant feature of MALT lymphoma pathologically. Continuing and slowly strengthening, a common feature of benign tumours, turned out minus RWO in four cases of parotid tumour-like BLEL.

Analysis of time–intensity curve types and the multiparameters

Yabuuchi et al[25] divided the parotid tumours into three categories: T_{max}> 210s and WR_{300} < 10% (PLA), T_{max}<60s and WR_{300} > 40% (Warthin's tumour) and 60s< T_{max}<100s and 10% < WR_{300} < 30% (malignant tumour). The TIC characteristics of PLA indicated late enhancing and continued growth type. Warthin's tumour presented early enhancing rapid declining and continued declining type. Malignant tumours presented as early enhancing and continued declining type. The degree of declining of Warthin's tumour was more than that of malignant tumour. Thus, according to TIC features and a comprehensive analysis of multiple parameters, PLA, Warthin's tumour and malignant tumour could all be differentiated.

According to the threshold values of TTP and ISI, this study divided TICs of parotid tumour-like BLEL and MALT lymphoma into three types: Type I (rapid increase and gradual type): TTP <79.65s, ISI> 0.807; Type II (gradual type): TTP> 79.65s, ISI <0.807; and Type III (late increase type): TTP> 79.65s, ISI> 0.807. Parotid tumour-like BLEL mainly presented as Type II (dominantly, 76.2%) and Type III, according to the characteristics of benign lesion. Five cases with the TICs of Type III might infer the evolution from tumour-like BLEL to MALT lymphoma. Parotid MALT lymphoma mainly presented as Type I (94.1%), in accordance with the characteristics of malignant tumour as high density of lymphoma cells. No significant difference in the late stage of enhancement (both draining out lightly) pathologically indicated the benign feature of tumour-like BLEL and a low-grade malignant feature of MALT lymphoma. Therefore, the characteristics of TIC, TTP and ISI had important significance in the

differential diagnosis of parotid tumour-like BLEL and MALT lymphoma.

The shortage of dynamic contrast-enhanced MR
The results showed that TTP, ISI and TIC types could provide important information for differential diagnosis. However, owing to the small amount of samples, we could not further analyse the clinical significance of four cases with TTS >30s in parotid tumour-like BLEL. We were also unable to further confirm the relationship between the TIC types and the evolution from parotid tumour-like BLEL to MALT lymphoma. A larger group of patients is needed for further analysis.

Conclusions

This study analysed five measured parameters (SI_{start}, TTS, SI_{max}, TTP and SI_{ending}), two calculated parameters (ISI and RWO) and TIC types in differential diagnosis between parotid tumour-like BLEL and MALT lymphoma. The results of this study are as follows: (1)

TTP can provide important information in the differential diagnosis between parotid tumour-like BLEL and MALT lymphoma, reflecting the pathological features; (2) the difference of SI_{start}, TTS, SI_{max} and SI_{ending} are not statistically significant and useless in differential diagnosis; (3) the significant difference in the ISI plays an important role in the differential diagnosis between the two lesions, and it also reflects the characteristics of MALT lymphoma such as early enhancement and rich blood supply; (4) the difference of mean RWO value is not statistically significant, reflecting the pathological feature as a low-grade malignancy of MALT lymphoma; and (5) parotid tumour-like BLEL mainly presented as Type II and Type III, with the majority of Type II. Parotid MALT lymphoma mainly presented as Type I. The classification of TIC types has a role in the differential diagnosis of these two lesions, providing important information.

Therefore, the parameters of DCE-MRI and TIC types can add much more important information for the differential diagnosis of parotid tumour-like BLEL and MALT lymphoma.

References

1. Sato K, Kawana M, Sato Y, Takahashi S. Malignant lymphoma in the head and neck associated with benign lymphoepithelial lesion of the parotid gland. *Auris Nasus Larynx* 2002; **29**: 209–14. doi: http://dx.doi.org/10.1016/S0385-8146(01)00144-4
2. Jordan RC, Speight PM. Lymphoma in Sjögren's syndrome. From histopathology to molecular pathology. *Oral Surg Oral Med Oral Pathol Oral Radiol Endod* 1996; **81**: 308–20. doi: http://dx.doi.org/10.1016/S1079-2104(96)80331-3
3. Abbondanzo SL. Extranodal marginal-zone B-cell lymphoma of the salivary gland. *Ann Diagn Pathol* 2001; **5**: 246–54. doi: http://dx.doi.org/10.1053/adpa.2001.26980
4. Schmid U, Helbron D, Lennert K. Development of malignant lymphoma in myoepithelial sialadenitis (Sjögren's syndrome). *Virchows Arch A Pathol Anat Histol* 1982; **395**: 11–43. doi: http://dx.doi.org/10.1007/BF00443482
5. DiGiuseppe JA, Corio RL, Westra WH. Lymphoid infiltrates of the salivary glands: pathology, biology and clinical significance. *Curr Opin Oncol* 1996; **8**: 232–7. doi: http://dx.doi.org/10.1097/00001622-199605000-00011
6. Tonami H, Ogawa Y, Matoba M, Kuginuki Y, Yokota H, Higashi K, et al. MR sialography in patients with Sjögren syndrome. *AJNR Am J Neuroradiol* 1998; **19**: 1199–203.
7. Tagnon BB, Theate I, Weynand B, Hamoir M, Coche EE. Long-standing mucosa-associated lymphoid tissue lymphoma of the parotid gland: CT and MR imaging findings. *AJR Am J Roentgenol* 2002; **178**: 1563–5. doi: http://dx.doi.org/10.2214/ajr.178.6.1781563
8. Habermann CR, Cramer MC, Graessner J, Gossrau P, Reitmeier F, Fiehler J, et al. Functional imaging of parotid glands: diffusion-weighted echo-planar MRI before and after stimulation. *Rofo* 2004; **176**: 1385–9. doi: http://dx.doi.org/10.1055/s-2004-813564
9. King AD, Yeung DK, Ahuja AT, Tse GM, Yuen HY, Wong KT, et al. Salivary gland tumors at *in vivo* proton MR spectroscopy. *Radiology* 2005; **237**: 563–9. doi: http://dx.doi.org/10.1148/radiol.2372041309
10. Laissy JP, Gaxotte V, Ironde-Laissy E, Klein I, Ribet A, Bendriss A, et al. Cardiac diffusion-weighted MR imaging in recent, subacute, and chronic myocardial infarction: a pilot study. *J Magn Reson Imaging* 2013; **38**: 1377–87. doi: http://dx.doi.org/10.1002/jmri.24125
11. Buisson A, Joubert A, Montoriol PF, Da Ines D, Hordonneau C, Pereira B, et al. Diffusion-weighted magnetic resonance imaging for detecting and assessing ileal inflammation in Crohn's disease. *Aliment Pharmacol Ther* 2013; **37**: 537–45. doi: http://dx.doi.org/10.1111/apt.12201
12. Hisatomi M, Asaumi J, Yanagi Y, Unetsubo T, Maki Y, Murakami J, et al. Diagnostic value of dynamic contrast-enhanced MRI in the salivary gland tumors. *Oral Oncol* 2007; **43**: 940–7. doi: http://dx.doi.org/10.1016/j.oraloncology.2006.11.009
13. Escott EJ, Rao VM, Ko WD, Guitierrez JE. Comparison of dynamic contrast-enhanced gradient-echo and spin-echo sequences in MR of head and neck neoplasms. *AJNR Am J Neuroradiol* 1997; **18**: 1411–9.
14. Medeiros LR, Duarte CS, Rosa DD, Edelweiss MI, Edelweiss M, Silva FR, et al. Accuracy of magnetic resonance in suspicious breast lesions: a systematic quantitative review and meta-analysis. *Breast Cancer Res Treat* 2011; **126**: 273–85. doi: http://dx.doi.org/10.1007/s10549-010-1326-9
15. Karim HT, Sparto PJ, Aizenstein HJ, Furman JM, Huppert TJ, Erickson KI, et al. Functional MR imaging of a simulated balance task. *Brain Res* 2014; **1555**: 20–7. doi: http://dx.doi.org/10.1016/j.brainres.2014.01.033
16. Junping W, Tongguo S, Yunting Z, Chunshui Y, Renju B. Discrimination of axillary metastatic from nonmetastatic lymph nodes with PROPELLER diffusion-weighted MR imaging in a metastatic breast cancer model and its correlation with cellularity. *J Magn Reson Imaging* 2012; **36**: 624–31. doi: http://dx.doi.org/10.1002/jmri.23695
17. Delongchamps NB, Beuvon F, Eiss D, Flam T, Muradyan N, Zerbib M, et al. Multiparametric MRI is helpful to predict tumor focality, stage, and size in patients diagnosed with unilateral low-risk prostate cancer. *Prostate Cancer Prostatic Dis.* 2011; **14**: 232–7. doi: http://dx.doi.org/10.1038/pcan.2011.9
18. Fathi Kazerooni A, Mohseni M, Rezaei S, Bakhshandehpour G, Saligheh Rad H. Multi-parametric (ADC/PWI/T2-w) image fusion approach for accurate semi-automatic segmentation of tumorous regions in glioblastoma multiforme. *MAGMA* 2015; **28**: 13–22. doi: http://dx.doi.org/10.1007/s10334-014-0442-7
19. O'Flynn EA, DeSouza NM. Functional magnetic resonance: biomarkers of response in breast cancer. *Breast Cancer Res* 2011; **13**: 204. doi: http://dx.doi.org/10.1186/bcr2815

20. Shah GV, Fischbein NJ, Patel R, Mukherji SK. Newer MR imaging techniques for head and neck. *Magn Reson Imaging Clin N Am* 2003; **11**: 449–69. doi: http://dx.doi.org/10.1016/S1064-9689(03)00069-2

21. Noworolski SM, Fischbein NJ, Kaplan MJ, Lu Y, Nelson SJ, Carvajal L, et al. Challenges in dynamic contrast-enhanced MRI imaging of cervical lymph nodes to detect metastatic disease. *J Magn Reson Imaging* 2003; **17**: 455–62. doi: http://dx.doi.org/10.1002/jmri.10280

22. Fischbein NJ, Noworolski SM, Henry RG, Kaplan MJ, Dillon WP, Nelson SJ. Assessment of metastatic cervical adenopathy using dynamic contrast-enhanced MR imaging. *AJNR Am J Neuroradiol* 2003; **24**: 301–11.

23. Tomura N, Omachi K, Sakuma I, Takahashi S, Izumi J, Watanabe O, et al. Dynamic contrast-enhanced magnetic resonance imaging in radiotherapeutic efficacy in the head and neck tumors. *Am J Otolaryngol* 2005; **26**: 163–7. doi: http://dx.doi.org/10.1016/j.amjoto.2004.11.011

24. Asaumi J, Yanagi Y, Konouchi H, Hisatomi M, Matsuzaki H, Kishi K. Application of dynamic contrast-enhanced MRI to differentiate malignant lymphoma from squamous cell carcinoma in the head and neck. *Oral Oncol* 2004; **40**: 579–84. doi: http://dx.doi.org/10.1016/j.oraloncology.2003.12.002

25. Yabuuchi H, Matsuo Y, Kamitani T, Setoguchi T, Okafuji T, Soeda H, et al. Parotid gland tumors: can addition of diffusion-weighted MR imaging to dynamic contrast-enhanced MR imaging improve diagnostic accuracy in characterization? *Radiology* 2008; **249**: 909–16. doi: http://dx.doi.org/10.1148/radiol.2493072045

26. Takashima S, Noguchi Y, Okumura T, Aruga H, Kobayashi T. Dynamic MR imaging in the head and neck. *Radiology* 1993; **189**: 813–21. doi: http://dx.doi.org/10.1148/radiology.189.3.8234709

27. Yabuuchi H, Fukuya T, Tajima T, Hachitanda Y, Tomita K, Koga M. Salivary gland tumors: diagnostic value of gadolinium-enhanced dynamic MR imaging with histopathologic correlation. *Radiology* 2003; **226**: 345–54. doi: http://dx.doi.org/10.1148/radiol.2262011486

28. Matsuzaki H, Yanagi Y, Hara M, Katase N, Asaumi J, Hisatomi M, et al. Minor salivary gland tumors in the oral cavity: diagnostic value of dynamic contrast-enhanced MRI. *Eur J Radiol* 2012; **81**: 2684–91. doi: http://dx.doi.org/10.1016/j.ejrad.2011.11.005